Oral Diseases (2004) 10, 94–98

http://www.blackwellmunksgaard.com

Oral and Maxillofacial Pathology

Dentine structure and mineralization in hypocalcified amelogenesis imperfecta: a quantitative X-ray histochemical study

MC Sánchez-Quevedo[1], G Ceballos[2], JM García[1], JD Luna[3], IA Rodríguez[4], A Campos[1]

[1]*Departamento de Histología, Facultad de Medicina y Odontología, Universidad de Granada, Granada, Spain;* [2]*Departamento de Estomatología, Hospital Clínico Universitario, Universidad de Granada, Granada, Spain;* [3]*Departamento de Bioestadística, Facultad de Medicina, Universidad de Granada, Granada, Spain;* [4]*Cátedra B de Histología y Embriología, Facultad de Odontología, Universidad Nacional de Córdoba, Córdoba, Argentina*

OBJECTIVE: This study was undertaken in order to establish the structural and mineralization pattern of the response of dentine to alterations in enamel in hypocalcified amelogenesis imperfecta (AI).
DESIGN: The images and data obtained with scanning electron microscopy and electron probe X-ray microanalysis in enamel and dentine specimens from control and affected teeth were compared in this study.
PATIENTS AND METHODS: We compared 46 fragments of permanent teeth from patients with clinically diagnosed hypocalcified AI and 20 normal permanent teeth. All specimens were prepared for electron probe X-ray microanalysis.
RESULTS: Dentine is characterized by thickening of the peritubular dentine and partial obliteration of the dentinal tubules that does not give rise to a compact sclerotic cast. In dentine, calcium levels were significantly higher in teeth with clinically hypocalcified AI in relation with control teeth ($P < 0.001$).
CONCLUSIONS: Dentine is affected in hypocalcified AI increasing mineralization (narrower tubules and higher content of calcium) in response to enamel disorder.
Oral Diseases (2004) **10**, 94–98

Keywords: tooth calcification; dentine; enamel; amelogenesis imperfecta

Introduction

Amelogenesis imperfecta (AI) represents a broad spectrum of genetic diseases affecting enamel formation in both primary and permanent dentitions (MacDougall *et al*, 2000). Three main clinical types of AI have been described. Its diverse clinical presentation is thought to be the result of specific genetic defects affecting the deposition, calcification and maturation of enamel. Although the structure and mineralization of enamel have been studied using different approaches in all three clinical types of AI (Wright, Robinson and Shore, 1991; Bäckman *et al*, 1993; Wright *et al*, 1993, 1995; Sánchez-Quevedo *et al*, 2001a,b; Seymen and Kiziltan, 2002), little is known about the structure and mineralization of dentine in AI.

Dentine, a mineralized hard tissue which forms the bulk of the tooth and gives it its characteristic shape, is not only the supporting structure of enamel, but is also the structure which, because of its particular mechanical properties, prevents the enamel from fracture. The microstructural features of enamel and dentine and the toughness of the dentine–enamel junction also contribute to crack resistance in the tooth (Craig and Peyton, 1958; Rasmussen, 1984; Lin and Douglas, 1994; Xu *et al*, 1998). During tooth germ development, enamel and dentine are interrelated: enamel proteins and dentine matrix proteins are involved in the process of dental biomineralization (Takano, Ozawa and Crenshaw, 1986; Hall *et al*, 1999; Paine *et al*, 2000). In this connection, amelogenins, which are secreted on the predentine surface, can interact with the cell surface of odontoblasts or with products secreted from the processes on the dentine–enamel surface. These events appear to be of importance for the development of teeth (Rajeswari *et al*, 1999). The fact that dentine is, in many teeth with AI, the surface exposed to the oral environment after the loss of the enamel, is also of interest to elucidate its structure and mineralization in this disorder.

The present study was designed to use quantitative X-ray microprobe analysis with scanning electron microscopy (SEM) as a histological approach to determine the

Correspondence: Prof. MC Sánchez-Quevedo, Departamento de Histología, Facultad de Medicina, Universidad de Granada, E-18071 Granada, Spain. Tel: 34 958 243514, Fax: 34 958 244034, E-mail: mcsanchez@histolii.ugr.es
Received 2 July 2003; revised 16 October 2003; accepted 27 October 2003

morphological patterns in dentine in hypocalcified AI – a clinical variety of AI – in which the enamel is frequently lost and the crown is composed mainly of dentine. In addition, we measured the contents of calcium in the dentine and compared it with calcium levels in the enamel. The use of SEM with electron-probe X-ray microanalysis (EPMA) to examine mineralized tissues is a productive tool for the histochemical study of both morphological features and the chemical elements that take part in the mineralization process (Engel and Hilding, 1984; Hals, Tveit and Totdal, 1988; Sánchez-Quevedo *et al*, 1989, 1998; Campos *et al*, 1994; López-Escámez *et al*, 1994). Only in the recent years a quantitative approach has been developed to investigate dental and other mineralized tissues with the peak-to-local-background (P/B) ratio method, using crystals of inorganic salts as standards (López-Escámez *et al*, 1993; Campos *et al*, 1994; Warley, 1997; Sánchez-Quevedo *et al*, 1998).

Information about the structure and mineralization of dentine in AI is of interest not only to establish the changes in the structural and mineralization pattern of dentine in response to enamel alterations, but also to establish how these patterns influence the outcome of restorative treatments now being explored for this disorder (Seow, 1993; Seow and Amaratunge, 1998).

Patients and methods

We studied the enamel and adjacent dentine in 46 permanent teeth fragments (Table 1) (15 incisors, 12 canines, 14 premolars and five molars) from four individuals (16–19 years old, members of the same family) with hypocalcified AI. All patients with AI were examined clinically and the diagnosis was confirmed by clinical examination and family history (Ceballos and Ceballos, 1988). The enamel in affected teeth was lusterless, opaque white to yellow-brown, and of normal extent; however, the crown was composed partially of dentine because the enamel had been lost in many teeth. AI specimens were obtained in the course of preparation for crown placement. No other clinical lesions were detected. The mode of inheritance was identified as autosomal dominant on the basis of traditional pedigree analysis for the AI trait. We used 20 normal tooth specimens (five incisors, five canines, five premolars and five molars) extracted during orthodontic or periodontal treatment as the control material. Analyses of the enamel and adjacent dentine in AI and control specimens were carried out in incisal margins and cusps.

Table 1 Distribution of teeth types in our materials

	Incisors	*Canines*	*Premolars*	*Molars*	*Total*
Controls	5	5	5	5	20
AI1	2	3		2	7
AI2	2	1	6		9
AI3	7	4	2	3	16
AI4	4	4	6		14
Total AI	15	12	14	5	46

Sample preparation for electron probe X-ray histochemical microanalysis

The tooth fragments were plunge-frozen in liquid nitrogen-cooled Freon 22. The samples were transferred to a Polaron E 5300 freeze-drying apparatus (Polaron Equipment Ltd, Weatford, UK) and dried at −80°C for 48 h. All specimens were mounted on a carbon stub and sputter-coated with a thin layer of carbon in an argon atmosphere at 0.1 Torr for 30 s.

Electron probe X-ray histochemical microanalysis

Specimens prepared as described above were studied using a Phillips XL-30 scanning electron microscope (Philips Electronics NV, Einthoven, The Netherlands) (operating voltage = 15 kV; spot size = 500 nm; tilt angle = 35°; take-off angle = 61.34°). An energy dispersive spectrometer (EDAX DX-4, EDAX International, Mahwah, NJ, USA) was used for quantitative analysis (count rate = 1200 counts per second; live time = 50 s). Spectra were collected by a pin-point electron beam at 40 000×. In each tooth, a total of 10 analyses were performed in enamel, and a further 10 analyses were carried out in dentine. A total of 920 analyses for AI (460 in enamel and 460 in dentine, from 46 teeth with AI) and 400 analyses for controls (200 in enamel and 200 in dentine, from 20 control teeth) were obtained. The P/B ratio method (Statham and Pawley, 1978; Small *et al*, 1979) was used to measure the content of calcium and phosphorus.

The microcrystalline salt standards used for calcium and phosphorus quantification (López-Escámez and Campos, 1994; Sánchez-Quevedo *et al*, 1998) were $Ca_2P_2O_7$, $C_6H_{11}O_7{\cdot}1/2Ca$, $CaHPO_4$, $Ca(H_2PO_4)_2$, $PO_4HCa{\cdot}2H_2O$, $C_{12}H_{21}O_{12}{\cdot}1/2Ca$, $CaH_4O_8P_2{\cdot}H_2O$, $CaSO_4{\cdot}2H_2O$. The standards were cryofixed in liquid N_2, freeze-dried and sputter-coated as described above, and analysed in the microscope immediately after preparation to avoid contamination or chemical modification. Microcrystalline standards were mounted on 200-mesh nickel grids fixed with adhesive graphite lamina to SEM holders. The elemental weight percent (WP) of each salt standard was calculated as reported in previous publications (Warley, 1993, 1997).

Morphological study

Carbon-coated specimens were gold-coated after EPMA analysis, and were examined in a Phillips XL-30 SEM and photographed.

Statistical study

Analysis of variance of the nested design was used with group, type of tooth and region as fixed factors, and individual, tooth and repetition of the analysis as random factors. Individual was nested within group, tooth was nested within individual, and repetition was nested within tooth.

The study design was analysed with a random effects model based on multilevel models; estimates were obtained with the residual maximum likelihood (REML) method.

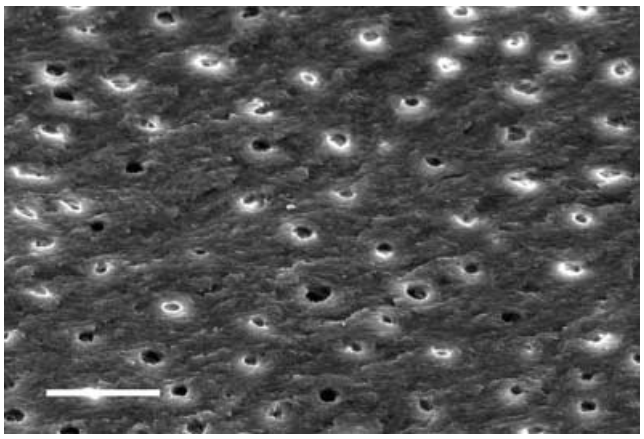

Figure 1 Narrowed lumina and partial obstruction of dentine tubules. The peritubular dentine around some lumina stands out as markedly paler areas. Scale bar 10 μm

Pairwise comparisons were performed using the Bonferroni method. All calculations were performed with S-Plus 2000 software (MathSoft, Seattle, WA, USA) within the linear mixed model procedure.

Results

Scanning electron microscopic images of dentine in teeth with clinically diagnosed hypocalcified AI showed dentine tubules with narrow, partly obliterated lumen. Peritubular dentine was clearly visible, although in many tubules the transition between peritubular and intratubular dentine could not be distinguished. No sclerotic casts were seen in the tubular lumina (Figures 1 and 2).

Table 2 presents the microanalytical data for calcium content in enamel and dentine from control and AI specimens for each type of tooth. Our results show no significant differences between the different samples of enamel analysed. The Ca/P ratio in AI enamel was 1.7 and the corresponding figure for control enamel was 1.8. We found significant differences for dentine ($P < 0.001$), with higher calcium contents in all four types of tooth with AI than in control teeth. The Ca/P ratio in dentine from AI and control teeth was 1.7. The comparisons in calcium levels in each tooth type between enamel and dentine show no significant differences for teeth with AI. In contrast, the enamel and dentine differed significantly in control teeth ($P < 0.01$), with higher contents of calcium appearing in the enamel.

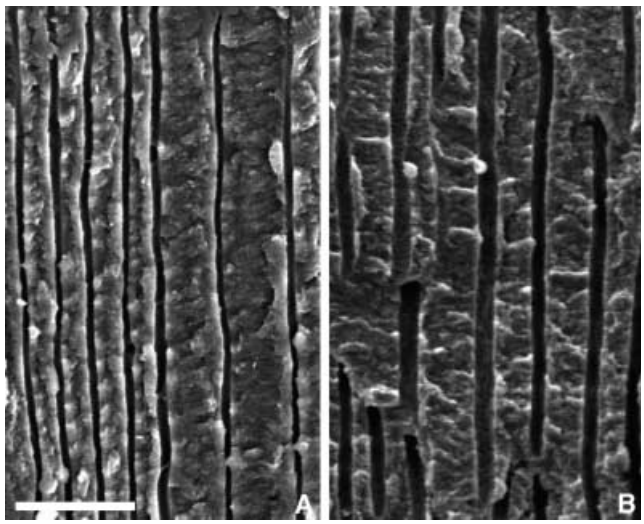

Figure 2 Narrowed dentine tubules (a) in comparison with control dentine tubules (b). No sclerotic casts are seen. Scale bar 20 μm

Discussion

Scanning electron microscopy has been used by different authors to identify morphological alterations in AI. These studies have focused on establishing the structure of enamel prisms and the rest of the structures related with them.

X-ray microanalytical histochemistry has been shown to be useful in revealing mineralization patterns in the enamel of teeth with AI (Wright *et al*, 1991; Sánchez-Quevedo *et al*, 2001a,b). However, few studies have attempted to elucidate the structure of dentine in AI and other enamel defects. The few reports published to date describe a wide range of anomalies, from minor defects to dentine dysplasia (Suzuki, Nakata and Eto, 1977; Nakata, Kimura and Bixler, 1985; Seymen and Kiziltan, 2002). To our knowledge, X-ray histochemical techniques have not been used to study the mineralization of dentine in AI.

Scanning electron microscopic images in our study revealed a morphological pattern of dentine characterized by thickening of the peritubular dentine and partial obliteration of the dentine tubules, but without the formation of compact sclerotic casts. The borderline between intertubular and peritubular dentine could not be distinguished easily in many tubules. Therefore this morphological pattern corresponds to the so-called

Table 2 Mean ± SD of calcium weight percentages in enamel and dentine of control and AI teeth

	Enamel		*Dentine*	
	Control	*AI*	*Control*	*AI*
Incisors	29.9 ± 1.8† (50)	33.1 ± 4.3 (150)	23.6 ± 1.7*† (50)	33.3 ± 3.6* (150)
Canines	30.2 ± 1.4† (50)	32.6 ± 3.3 (120)	24.9 ± 1.4*† (50)	32.5 ± 3.5* (120)
Premolars	31.2 ± 2.2† (50)	32.7 ± 3.2 (140)	24.8 ± 1.9*† (50)	33.7 ± 4.0* (140)
Molars	34.0 ± 3.0† (50)	34.3 ± 4.4 (50)	27.9 ± 1.8*† (50)	33.2 ± 3.6* (50)

The number of analysis appears in parenthesis.
Results of the comparison in each type of tooth: *$P < 0.001$, †$P < 0.01$.

sclerotic dentine, i.e. the morphological transformation observed with SEM when dentine is exposed to the oral environment, as frequently seen in hypocalcified AI (Van Meerbeek *et al*, 1994).

The use of X-ray microanalytical histochemistry to study hard tissues has been a combination of mostly qualitative and semiquantitative methods (Wright *et al*, 1991; Warley, 1993). These studies, which have been useful in establishing different patterns of mineralization in hard tissues, have nonetheless failed to find significant differences in the mean calcium levels between normal and AI teeth, and suggested that the mineral in both cases is probably similar, at least in primary composition. Internal variations in calcium levels in the thickness of the enamel have been reported, and the nature of qualitative X-ray microprobe analysis is such that it causes different degrees of tissue excitation depending on tissue density. Bäckman *et al* (1993), who used secondary ion mass spectrometry, were also unable to distinguish between the clinical phenotypes of AI suggesting that a rather different clinical appearance reflects a difference in the expressivity of the disturbance.

Quantitative X-ray microanalytical histochemistry provides accurate measurements of elements involved in mineralization, and overcomes the limitations of qualitative and semiquantitative techniques. In previous reports we established the suitability and precision of quantitative X-ray techniques to analyse mineralized tissues, including enamel and dentine (Sánchez-Quevedo *et al*, 1998, 2001a,b). The recent development of crystal salt standards for the analysis of mineralized structures such as the otoconia, which consist mainly of calcium carbonate, has made it possible to overcome some problems related with the quantification of hard tissues with EPMA.

Our quantitative X-ray microanalytical study failed to find any statistically significant differences between the levels of calcium in enamel from control and AI teeth. However, we did find statistically significant differences between calcium levels in the dentine from AI and control within the same type of tooth. Although the Ca/P ratio is lower (1.7) than in normal enamel (1.8–2.2) and enamel from teeth with other types of AI (1.9–2.1) (Wright *et al*, 1991) our results once again point to the need – as suggested by Bäckman *et al*, 1993 – to re-examine the presumed correlation between clinical phenotypes and the exact amounts of mineral elements as measured with different analytical procedures. Hypermineralization of dentine has been related with morphological features, i.e. sclerotic dentine, which is known to be harder that orthodentin (Grajower, Azaz and BronLevi, 1977). These images are therefore more likely to reflect the higher mineralization of dentine than the hypomineralization of enamel. It remains to be determined whether increased enamel proteins in hypocalcified AI amelogenins and non-amelogenins, which interact with dentine matrix protein and are involved in growing of mineral crystal, play a role in this process (Wright *et al*, 1992; Rajeswari *et al*, 1999).

The structural features and mineralization data for dentine in hypocalcified AI should be interpreted as mechanisms of response to the defective, friable enamel that is frequently lost. But these structural features and mineralization are also of interest because bonding to dentine in AI differs significantly from bonding to unaffected normal dentine. It is reasonable to predict that dentine adhesives will be less effective when applied to sclerotic dentine than to unaffected normal dentine (Van Meerbeek *et al*, 1994). In addition, etching techniques used for hypermineralized dentine should also be reviewed and modified (Kwong *et al*, 2000).

Acknowledgements

This study was supported in part by Ministry of Education and Culture through Project no. PB97-0804, and by the Agencia Española de Cooperación Internacional through Project AECI/98/01. We thank M. Ángeles Robles for her competent technical assistance.

References

Bäckman B, Lundgren T, Urban Engström U *et al* (1993). The absence of correlations between a clinical classification and ultrastructural findings in amelogenesis imperfecta. *Acta Odontol Scand* **51:** 79–89.

Campos A, López-Escámez JA, Crespo PV *et al* (1994). Gentamicin ototoxicity in otoconia: quantitative electron probe X-ray microanalysis. *Acta Otolaryngol (Stockh)* **114:** 18–23.

Ceballos A, Ceballos G (1988). Estudio de una familia con amelogenesis imperfecta. *Adv Odontoestomatol* **4:** 125–128.

Craig RG, Peyton FA (1958). The microhardness of enamel and dentine. *J Dent Res* **37:** 661–668.

Engel MB, Hilding OH (1984). Mineralization of developing teeth. *Scanning Electron Microsc* **4:** 1833–1845.

Grajower R, Azaz A, BronLevi M (1977). Microhardness of sclerotic dentin. *J Dent Res* **56:** 446.

Hall R, Septier D, Embery G *et al* (1999). Stromelysin-1 (MMP-3) in forming enamel and predentine in rat incisor-coordinated distribution with proteoglycans suggests a functional role. *Histochemistry J* **31:** 761–770.

Hals E, Tveit AV, Totdal B (1988). X-ray microanalysis of dentin: a review. *Scanning Microsc* **2:** 357–369.

Kwong SM, Tay FR, Yip HK *et al* (2000). An ultrastructural study of the application of dentine adhesives to acid-conditioned sclerotic dentine. *J Dent* **28:** 515–528.

Lin CP, Douglas WH (1994). Structure-property relations and crack resistance at the bovine dentin-enamel junction. *J Dent Res* **73:** 1072–1078.

López-Escámez JA, Campos A (1994). Standards for X-ray microanalysis of calcified structures. *Scanning Electron Microsc* **8:** 171–185.

López-Escámez JA, Crespo PV, Cañizares FJ *et al* (1993). Standards for quantification of elements in the otolithic membrane by electron probe x-ray microanalysis: calibration curves and electron beam sensitivity. *J Microsc* **171:** 215–222.

López-Escámez JA, Cañizares FJ, Crespo PV *et al* (1994). Electron probe microanalysis of gentamicin-induced changes on ionic composition of the vestibular gelatinous membrane. *Hearing Res* **76:** 60–66.

MacDougall M, Simmons D, Gu TT *et al* (2000). Cloning, characterization and immunolocalization of human ameloblastin (Ambn). *Eur J Oral Sci* **108:** 303–310.

Nakata M, Kimura O, Bixler D (1985). Interradicular dentin dysplasia associated with amelogenesis imperfecta. *Oral Surg Oral Med Oral Pathol* **60:** 182–187.

Paine CT, Paine ML, Luo W *et al* (2000). A tuftelin-interacting protein (TIP39) localizes to the apical secretory pole of mouse ameloblasts. *J Biol Chem* **275:** 22284–22292.

Rajeswari MH, Ravindranath RM, Moradian-Oldak J *et al* (1999). Tyrosyl motif in amelogenins binds N-acetyl-D-glucosamine. *J Biol Chem* **274:** 2464–2471.

Rasmussen ST (1984). Fracture properties of human teeth in proximity to the dentinoenamel junction. *J Dent Res* **63:** 1362–1368.

Sánchez-Quevedo MC, Crespo PV, García JM *et al* (1989). X-ray microanalytical histochemistry of human circumpulpar and mantle dentine. *Bone Mineral* **6:** 323–329.

Sánchez-Quevedo MC, Nieto-Albano OH, García JM *et al* (1998). Electron probe microanalysis of permanent human enamel and dentine. A methodological and quantitative study. *Histol Histopathol* **13:** 109–113.

Sánchez-Quevedo MC, Ceballos G, García JM *et al* (2001a). Quantitative analytical electron microscopy of calcium in hypocalcified amelogenesis imperfecta. *Scanning* **23:** 152–153.

Sánchez-Quevedo MC, Ceballos G, García JM *et al* (2001b). Scanning electron microscopy and calcification in amelogenesis imperfecta in anterior and posterior human teeth. *Histol Histopathol* **16:** 827–832.

Seow WK (1993). Clinical diagnosis and management strategies of amelogenesis imperfecta variants. *Pediatr Dentistry* **15:** 384–393.

Seow WK, Amaratunge FA (1998). The effects of acid-etching on enamel from different clinical variants of amelogenesis imperfecta: a SEM study. *Pediatr Dentistry* **20:** 37–42.

Seymen F, Kiziltan B (2002). Amelogenesis imperfecta: a scanning electron microscopic and histopathologic study. *J Clin Pediatr Dent* **26:** 327–335.

Small JA, Heinrich KFJ, Newbury DE *et al* (1979). Progress in the development of the peak-to-background method for the quantitative analysis of single particles with the electron probe. *Scanning Electron Microsc* **II:** 807–816.

Statham PJ, Pawley JB (1978). A new method for particle X-ray microanalysis on peak to background measurements. *Scanning Electron Microsc* **1:** 469–478.

Suzuki S, Nakata M, Eto K (1977). Clinical and histologic observations of opalescent dentin associated with enamel defects. *Oral Surg Oral Med Oral Pathol* **44:** 767–774.

Takano Y, Ozawa H, Crenshaw MA (1986). Ca-ATPase and ALPase activities at the initial calcification sites of dentin and enamel in the rat incisor. *Cell Tissue Res* **243:** 91–99.

Van Meerbeek B, Braem M, Lambrechts P *et al* (1994). Morphological characterization of the interface between resin and sclerotic dentine. *J Dent* **22:** 141–146.

Warley A (1993). Quantitative X-ray microanalysis of thin sections in biology appraisal and interpretation of results. In: Sigee DC, Morgan AJ, Sumner AT, Warley A, eds. *X-ray Microanalysis in Biology*. *Experimental Techniques and Applications*. Cambridge University Press: Cambridge, pp. 47–57.

Warley A (1997). *X-ray Microanalysis for Biologists*. Portland Press: London.

Wright JT, Robinson C, Shore R (1991). Characterization of the enamel ultrastructure and mineral content in hypoplastic amelogenesis imperfecta. *Oral Surg Oral Med Oral Pathol* **72:** 594–601.

Wright JT, Lord V, Robinson C, Shore R (1992). Enamel ultrastructure in pigmented hypomaturation amelogenesis imperfecta. *J Oral Pathol Med* **21:** 390–394.

Wright JT, Duggal MS, Robinson C, Kirkham J, Shore R (1993). The mineral composition and enamel ultrastructure of hypocalcified amelogenesis imperfecta. *J Craniofac Genet Dev Biol* **13:** 117–126.

Wright JT, Deaton TG, Hall KI *et al* (1995). The mineral and protein content of enamel in amelogenesis imperfecta. *Conn Tiss Res* **32:** 247–252.

Xu HHK, Smith DT, Jahanmir S *et al* (1998). Indentation damage and mechanical properties of human enamel and dentine. *J Dent Res* **77:** 472–480.